Electronic Supplementary Information

Modulating Interleaved ZnO Assembly with CuO Nanoleaves for Multifunctional Performance: Perdurable CO_2 Gas Sensor and Visible Light Catalyst

*Shravanti Joshi [a, b, c], Ram Kumar C. B. [a, c, d], Lathe Jones [a, c], Edwin L. H. Mayes [e], Samuel J. Ippolito [a, c, d], and Manorama V. Sunkara [b, c]**

[a] Centre for Advanced Materials and Industrial Chemistry (CAMIC), School of Science, College of Science, Engineering & Health, RMIT University, Melbourne, VIC 3001, Australia.

[b] Nanomaterials Laboratory, Inorganic & Physical Chemistry Division, CSIR-Indian Institute of Chemical Technology, Hyderabad 500007, India. **E-mail:** manorama@iict.res.in, **Tel.:** +91 40 27193225, **Fax:** +91 40 27160921.

[c] RMIT-IICT Research Centre, CSIR-Indian Institute of Chemical Technology, Hyderabad - 500007, India.

[d] School of Engineering, College of Science, Engineering & Health, RMIT University, Melbourne, VIC 3001, Australia.

[e] RMIT Microscopy and Microanalysis Facility (RMMF), RMIT University, Melbourne, Victoria 3001, Australia

**To whom all Correspondences should be addressed.*

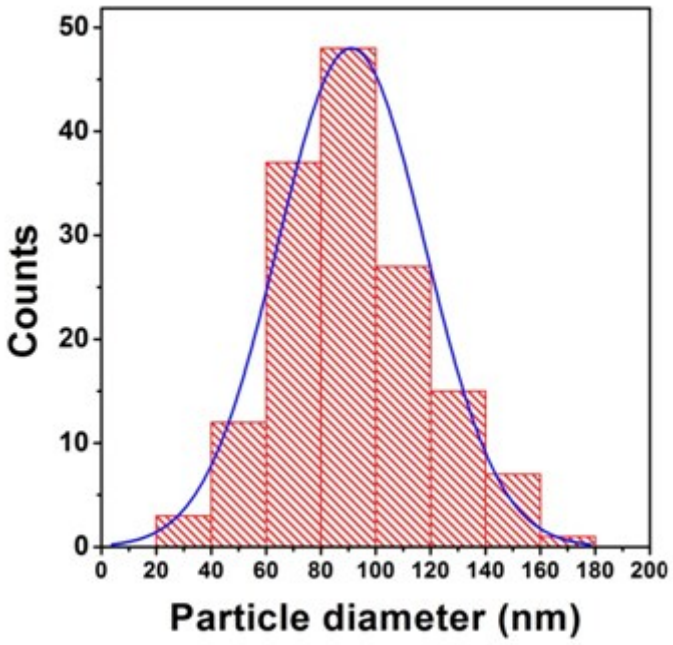

Figure S1.a Particle size distribution calculated from FE-SEM image (N-150 particles) given in Fig. 1h illustrating hierarchical ZnO spheres synthesized at 500°C for 2 h.

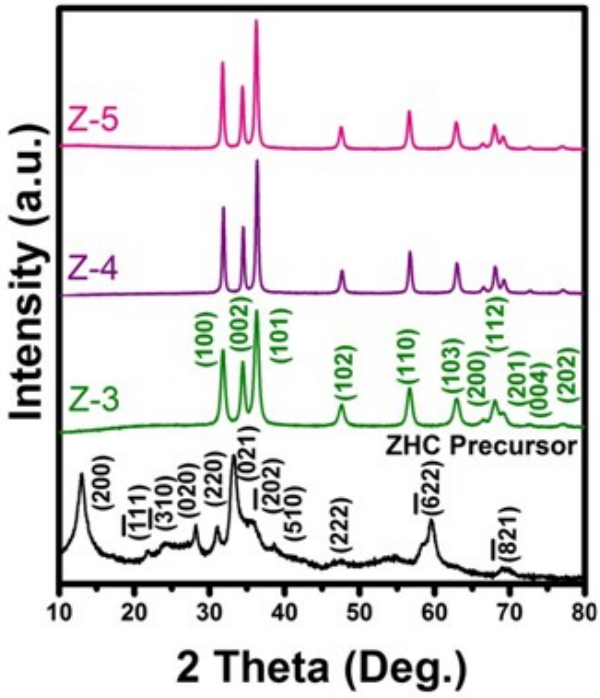

Figure S1.b X-ray diffractograms of Zinc hydroxide carbonate (ZHC) precursor synthesized at 120°C for 6 h, ZnO calcined at 300°C (Z-3), 400°C (Z-4) and 500°C (Z-5) for 2 h.

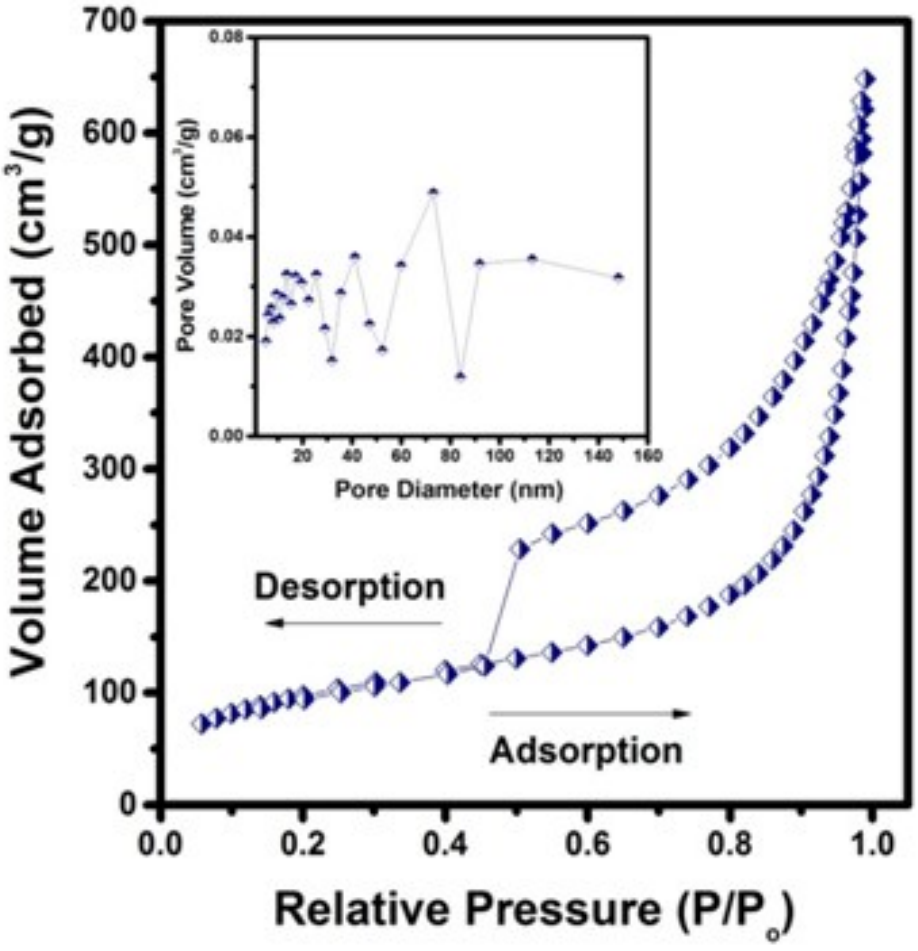

Figure S2 Nitrogen adsorption–desorption isotherms ZnO microspheres (Z-4). **Inset** pore size distribution curve.

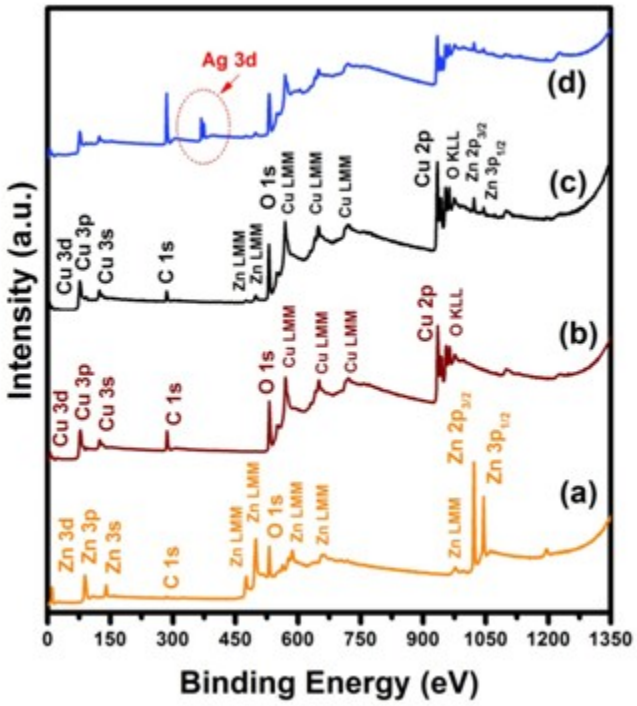

Figure S3 Representative **s**tacked XPS spectrum of **(a)** pure ZnO, **(b)** pure CuO, **(c)** CZ-1:1 and **(d)** 1 wt%Ag-CZ-1:1.

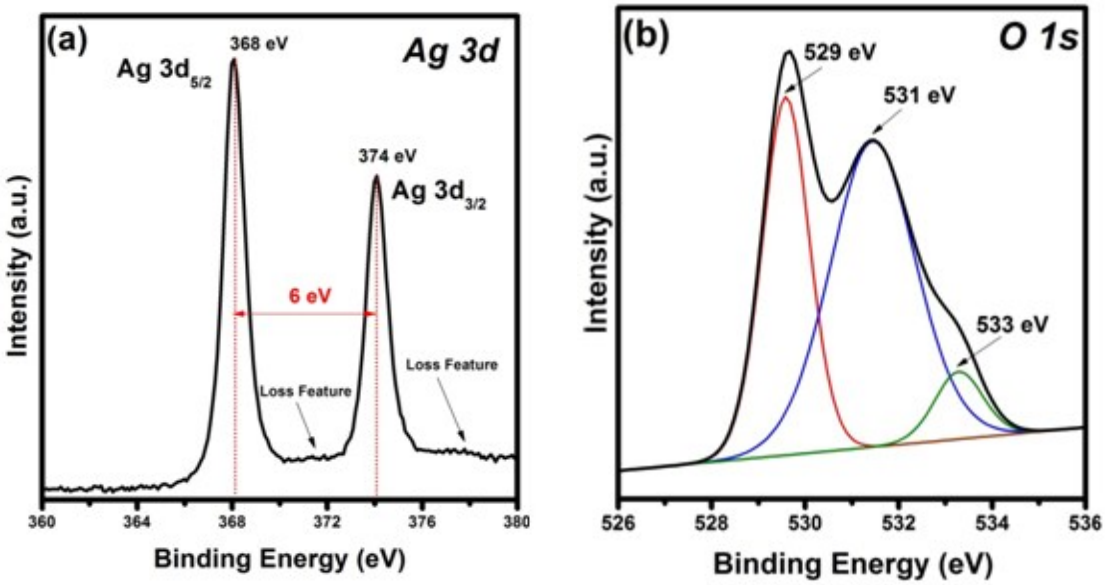

Figure S4 XPS core level spectra of 1 wt.%Ag-CZ-1:1,where **(a)** Ag 3d and **(b)** O 1s.

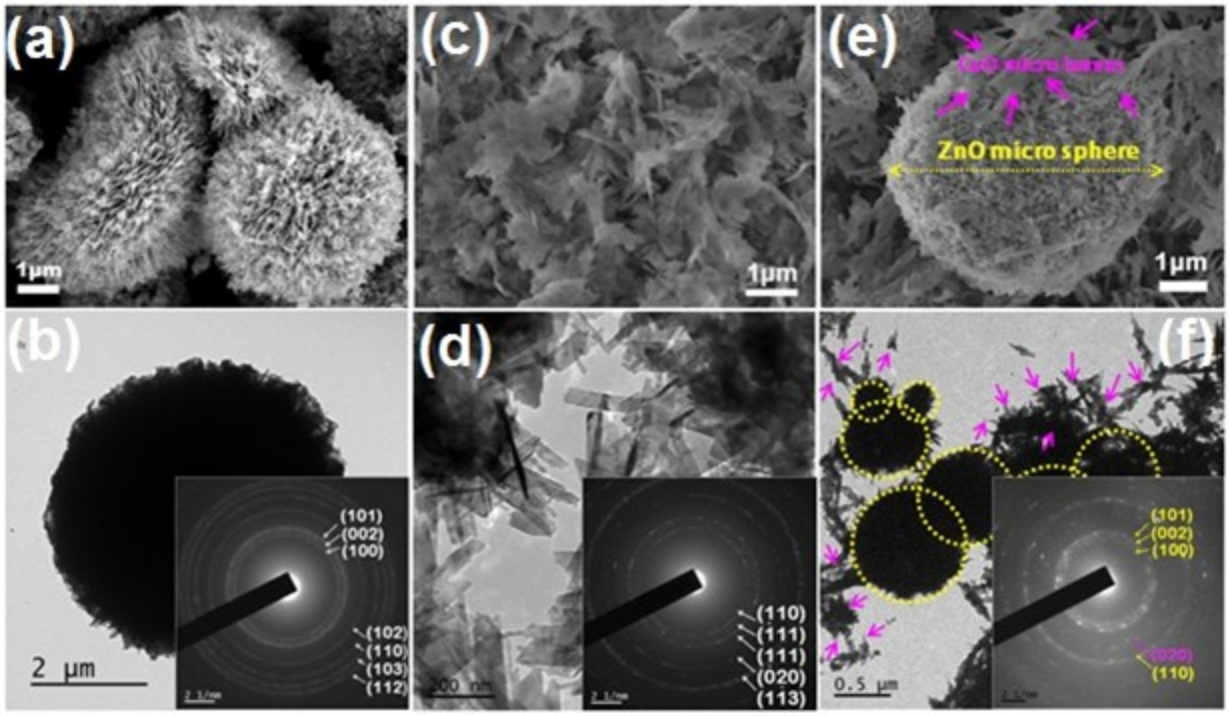

Figure S5 FE-SEM and TEM micrographs of **(a-b)** pure ZnO obtained at 400^{o}C for 2 h, **(c-d)** pure CuO obtained at 50^{o}C for 12 h and **(e-f)** CuO/ZnO composite in 1:8 mole ratio (CZ-1:8) obtained at 50^{o}C for 12 h. The inset in each case represents the corresponding SAED pattern. Pink arrows and yellow circles represent CuO nanoleaves and ZnO spheres respectively.

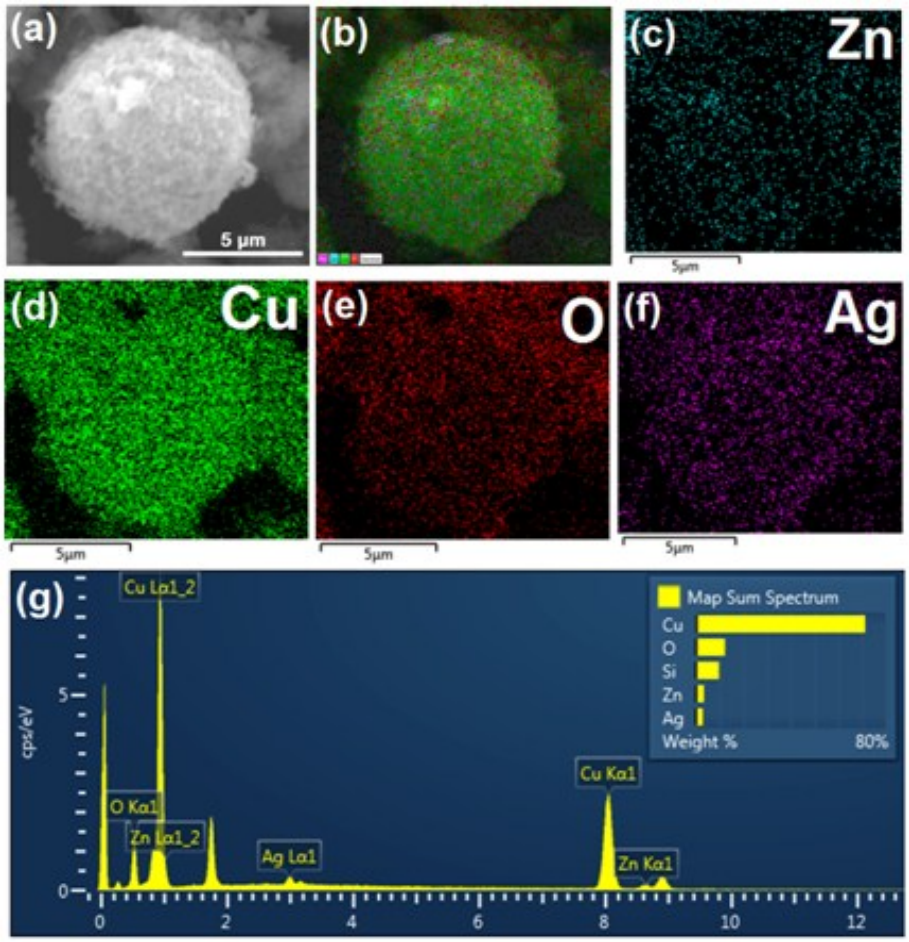

Figure S6 (a) Scanning electron micrograph reveals the actual area of CuO/ZnO composite used for elemental quantification, **(b)** layered EDS micrograph, elemental maps demonstrate uniform presence of **(c)** zinc (Zn), **(d)** copper (Cu), **(e)** oxygen (O), **(f)** silver (Ag) and **(g)** energy dispersive X-ray spectroscopy analysis of CuO/ZnO (CZ-1:1) decorated with 5 wt.%Ag.

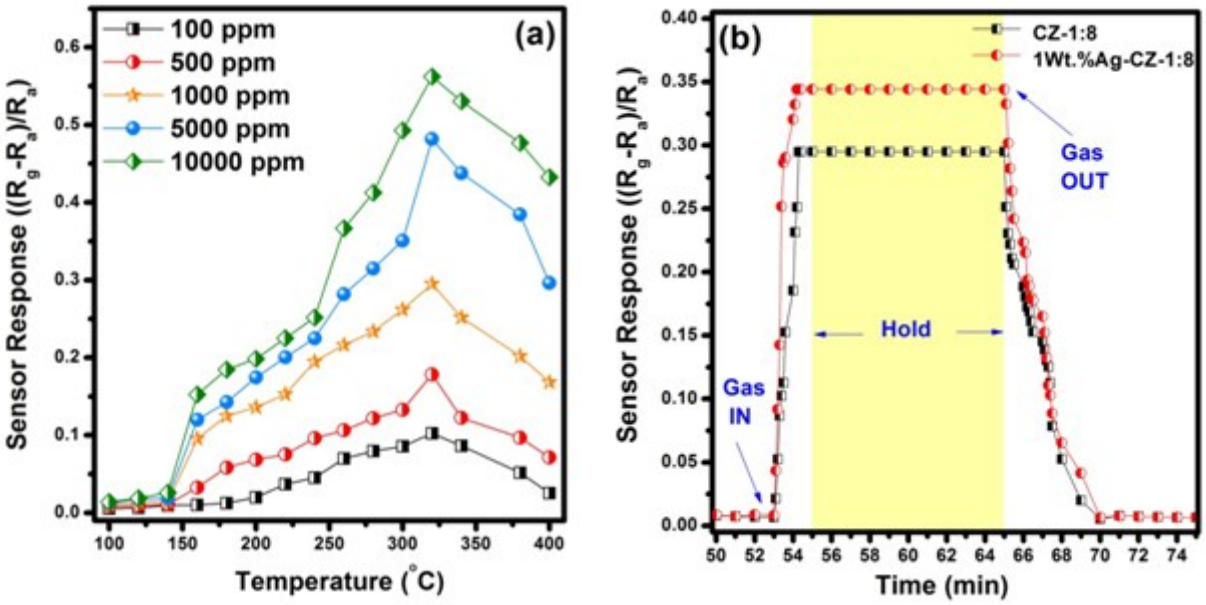

Figure S7 (a) Sensor response characteristics of CZ-1:8 composite as a function of operating temperature towards different CO_2 gas concentrations and **(b)** response/recovery curves for composites towards 1000 ppm CO_2 gas at 320^{o}C.

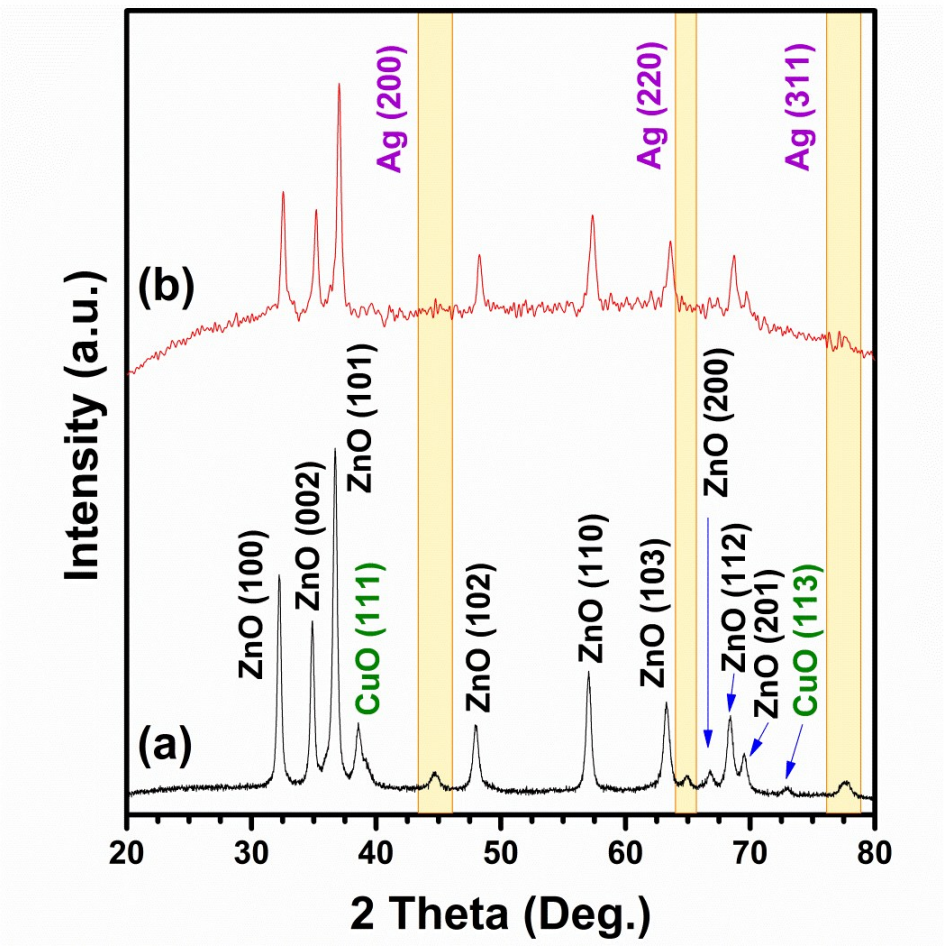

Figure S8.a X-ray diffractograms of 1 wt.%Ag-CZ-1:8 composite where **(a)** before and **(b)** after 40 days of continuous sensing performance towards 1000 ppm CO_2 gas balanced in dry air at 320^{o}C.

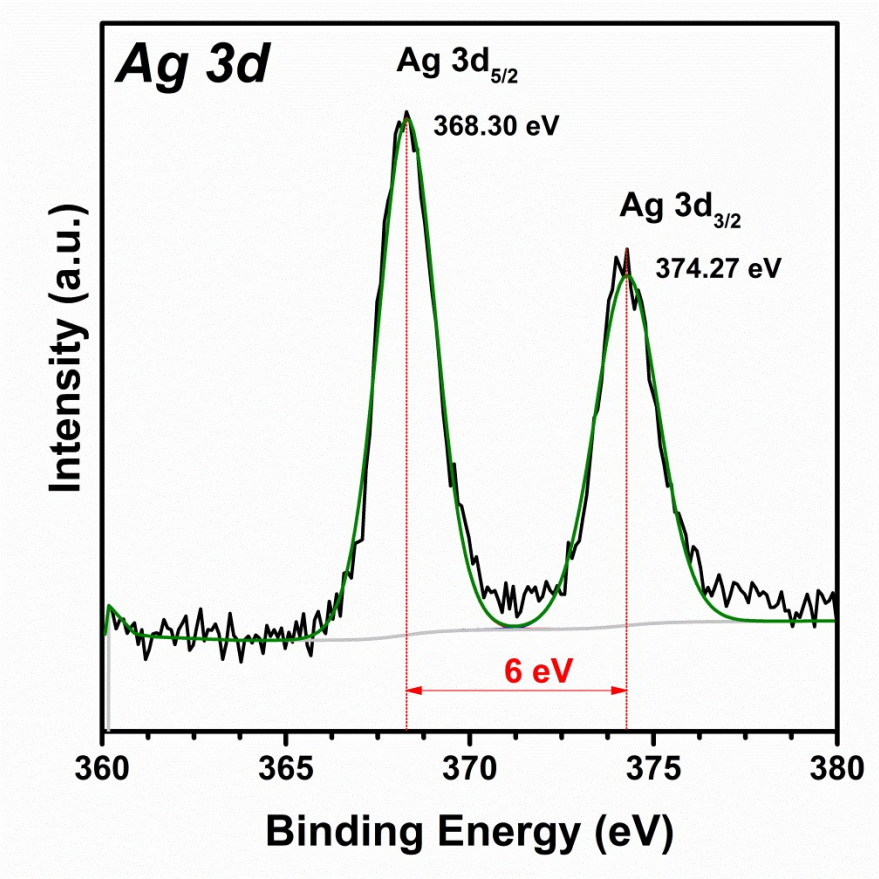

Figure S8.b XPS core level spectrum of Ag after 40 days of continuous sensing performance towards 1000 ppm CO_2 gas balanced in dry air at 320^{o}C.

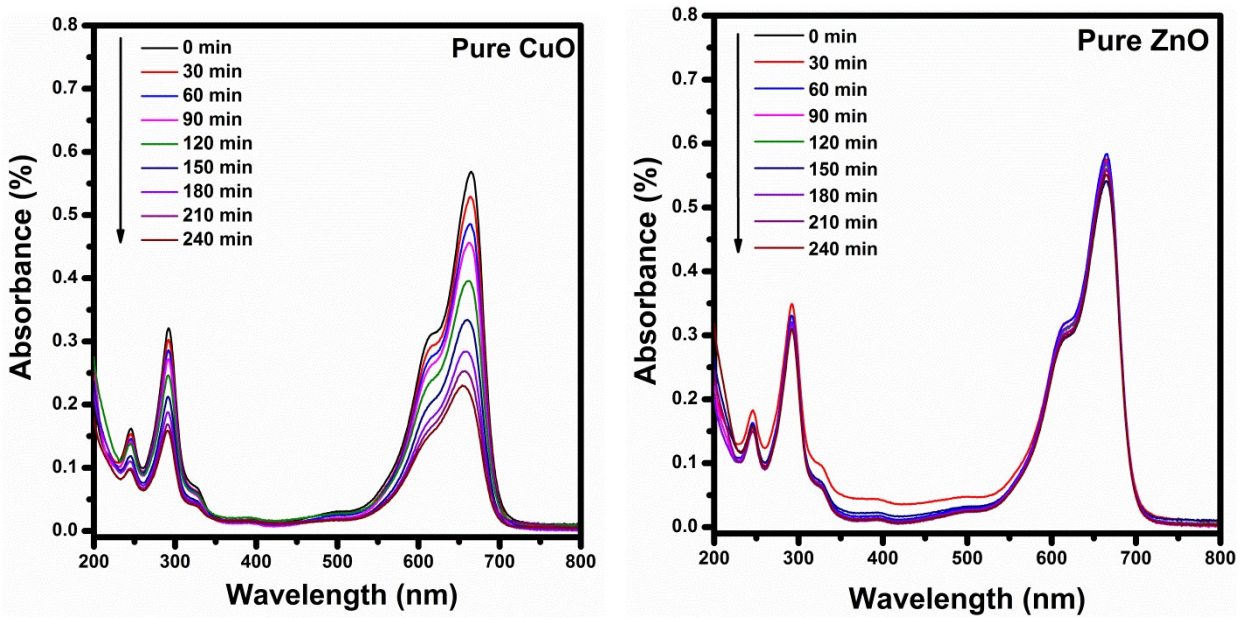

Figure S9 UV-Vis absorbance spectra depicting the change in concentration of MB under visible irradiation as a function of time for various photocatalyst.

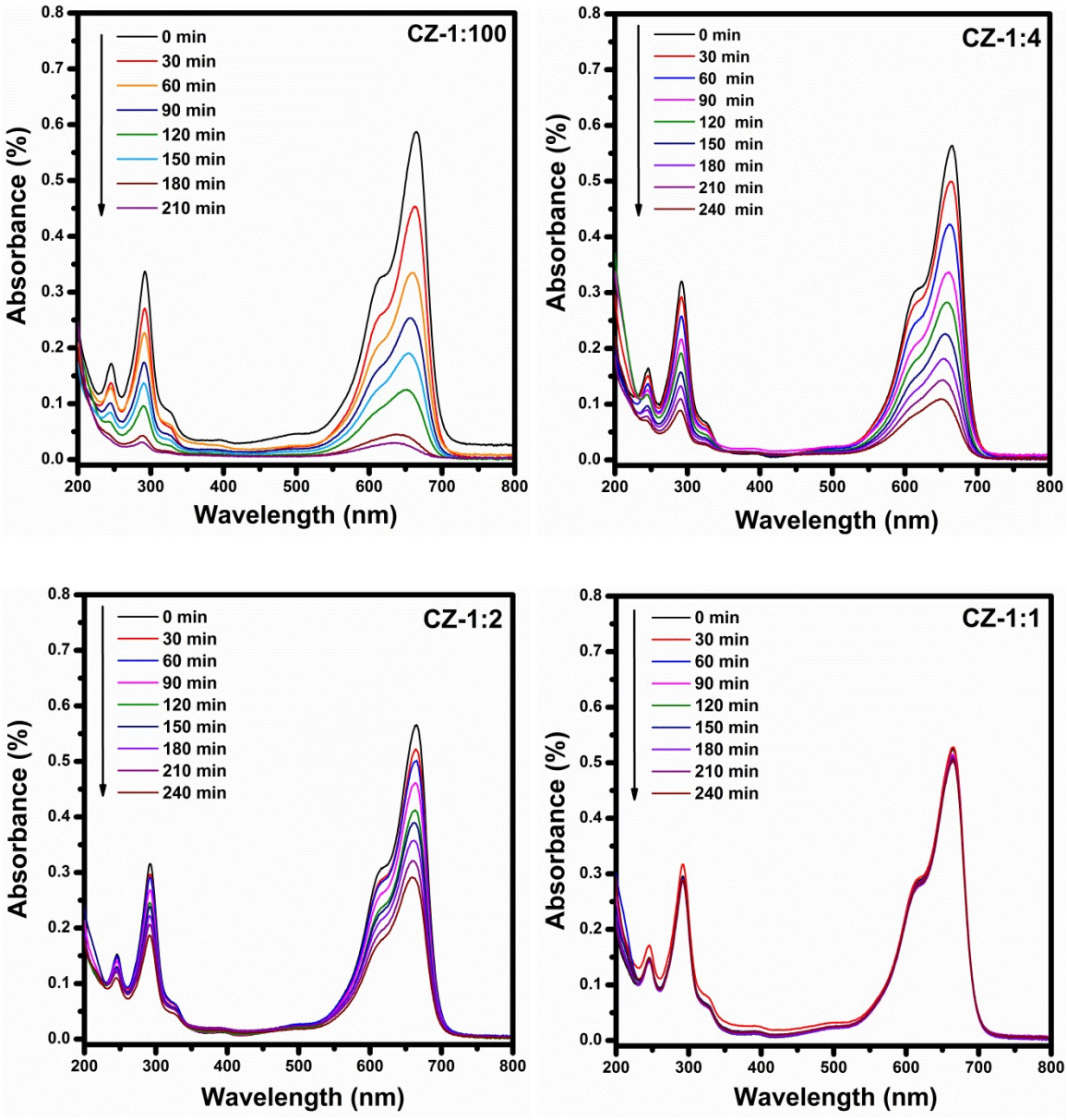

Figure S10 UV-Vis absorbance spectra depicting the change in concentration of MB under visible irradiation as a function of time for various photocatalyst.

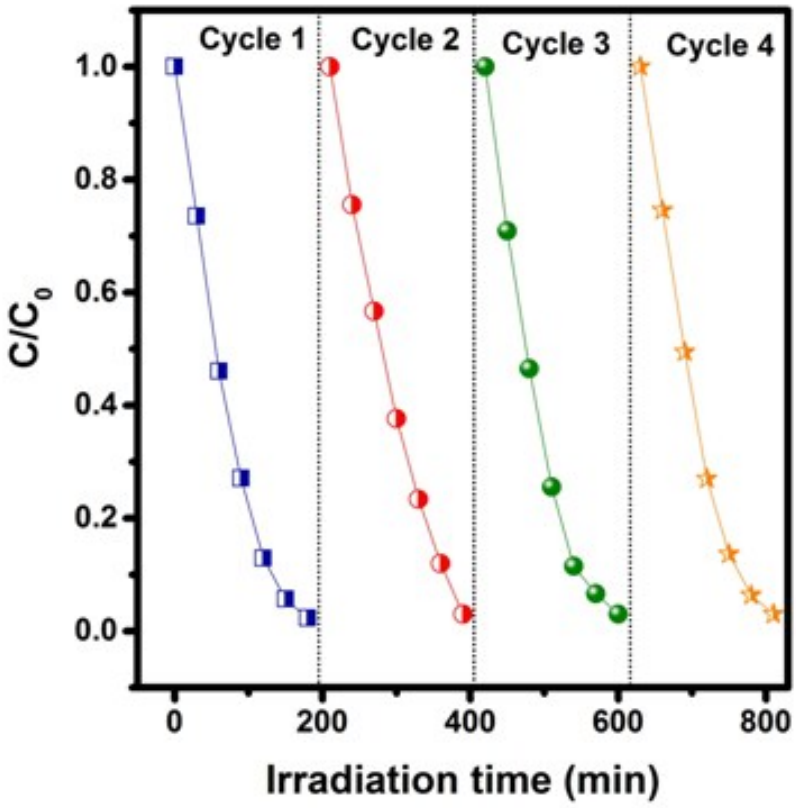

Figure S11.a Chemical stability testing of the CZ-1:8 interleaved assembly under visible light irradiation for four consecutive cycles.

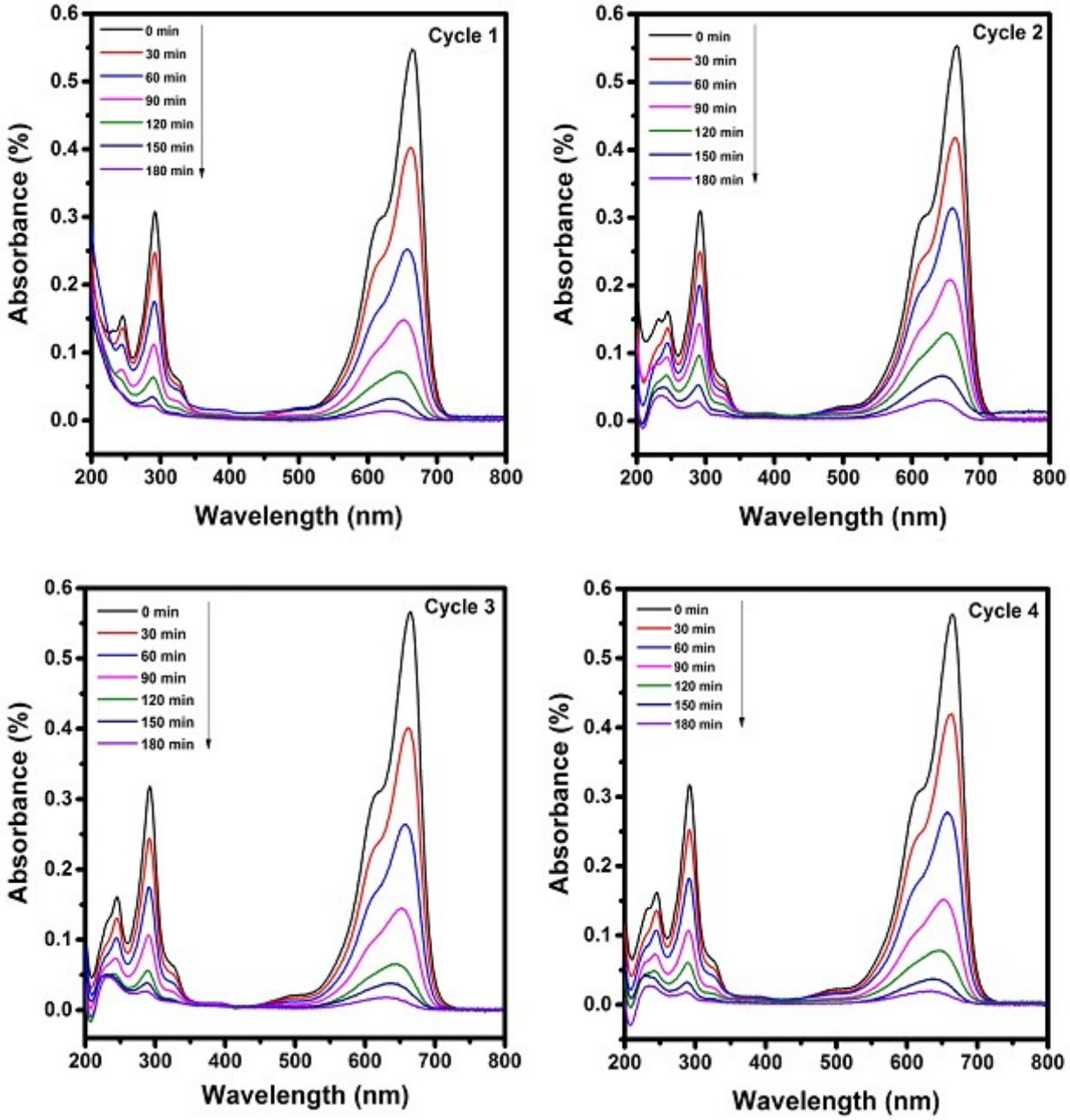

Figure S11.b Rate of photocatalytic degradation of MB under visible light irradiation in presence of CZ-1:8 for four consecutive cycles.

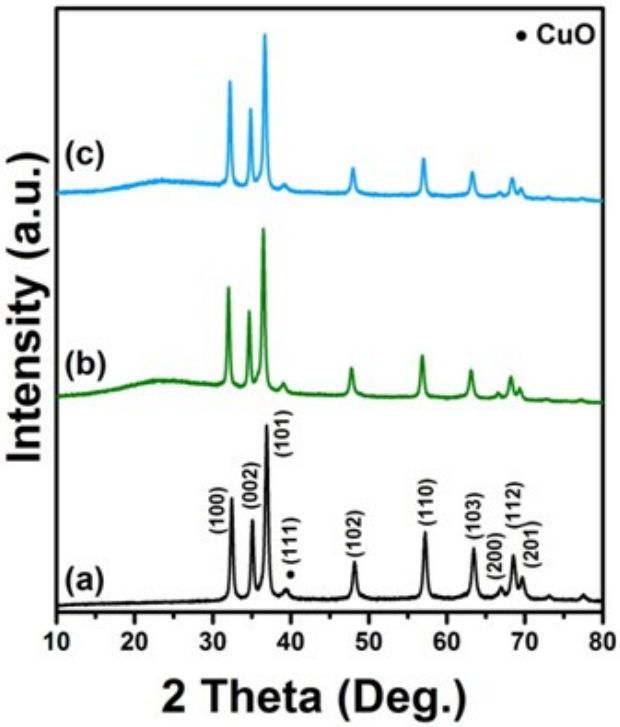

Figure S12 X-ray diffractograms where **(a)** as-synthesized CZ-1:8 composite, **(b)** after 40 days of CO_2 gas sensing performance and **(c)** after 4 consecutive cycles of visible light induced MB degradation.

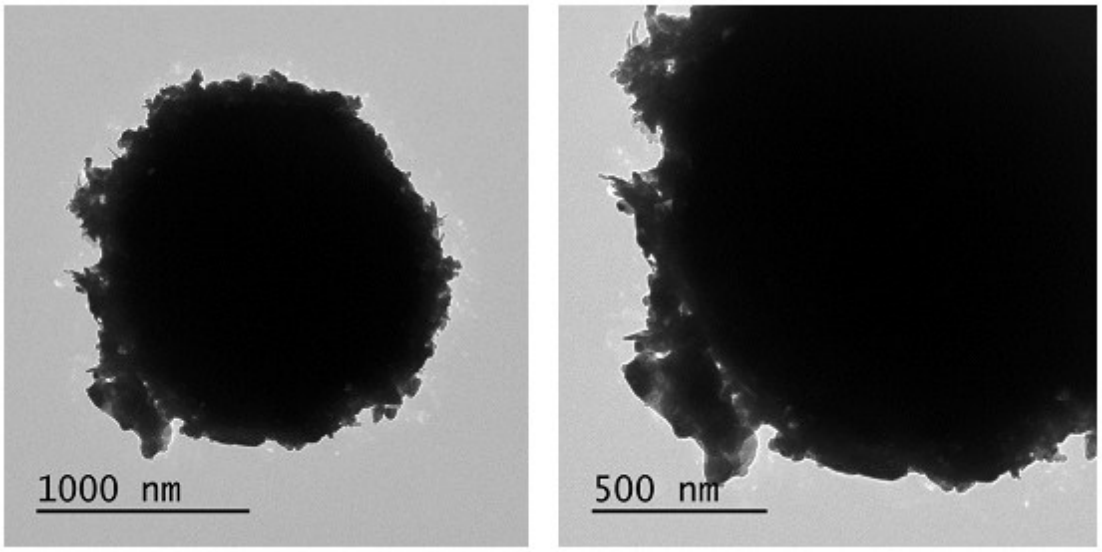

Figure S13 TEM micrograph of CZ-1:8 composite after 40 days of continuous CO_2 gas sensing test.

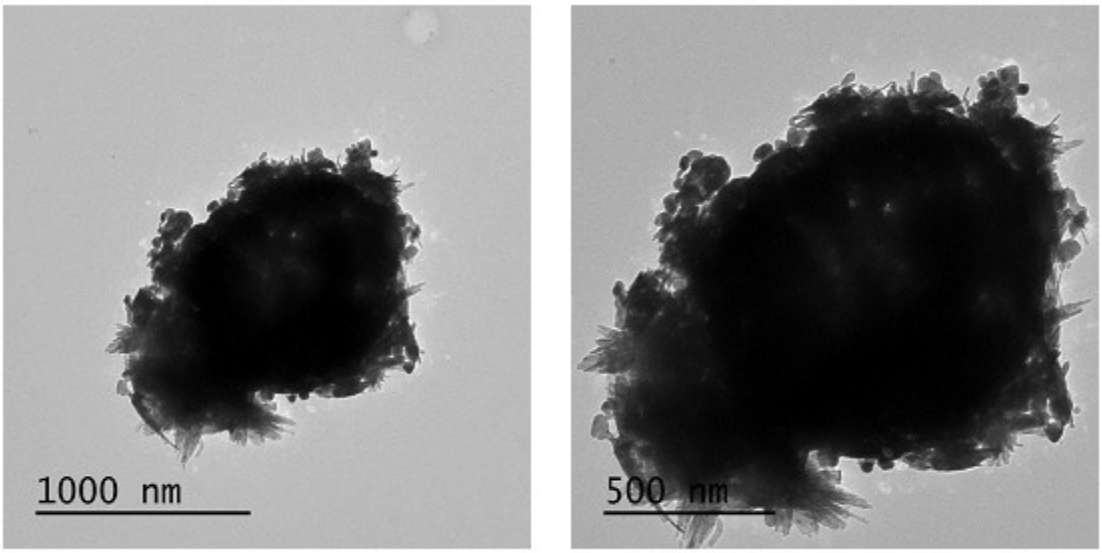

Figure S14 TEM micrograph of CZ-1:8 composite after 4 consecutive photocatalytic cycles of MB degradation studies.